Electronic Supplementary Material (ESI) for RSC Advances

Supplemental Material

For

Cation non-stoichiometry in "$CaCu_3Ti_4O_{12}$" (CCTO) ceramics

Rainer Schmidt[1,*], Shubhra Pandey[2,3], Patrick Fiorenza[4], Derek C. Sinclair[2]

[1] *Universidad Complutense de Madrid, Departamento. Física Aplicada III, GFMC, Facultad de Ciencias Físicas, 28040 Madrid, Spain*

[2] *The University of Sheffield, Materials Science and Engineering, Mappin Street, Sheffield S1 JD, United Kingdom*

[3] *Indian Institute of Technology Kanpur, Department of Materials Science and Engineering, Kalyanpur, Kanpur - 208 016, India*

[4] *CNR-IMM, Strada VIII n.5, Zona Industriale, 95121 Catania, Italy*

* Corresponding author. Email: rainerxschmidt@googlemail.com

Part I.) Phase Analysis

(a)XRD phase analysis

(b) Phase analysis by Scanning Electron Microscopy (SEM)

(c) Scanning Tunneling Microscopy (STM)

Part II.) Analysis of impedance spectroscopy data using ε' vs f and M'' vs f plots

(a) Impedance spectra from Cu deficient compositions 1 – 4

(b) Impedance spectra from compositions 5 – 8 containing secondary CuO

I. Phase analysis

(a) XRD phase analysis

Supporting Material (SM) Figures 1&2 present the powder XRD patterns of all compositions 1 – 8 from the phase diagram (Fig.1 main text), heat treated at 1000 ºC and 1100 ºC.

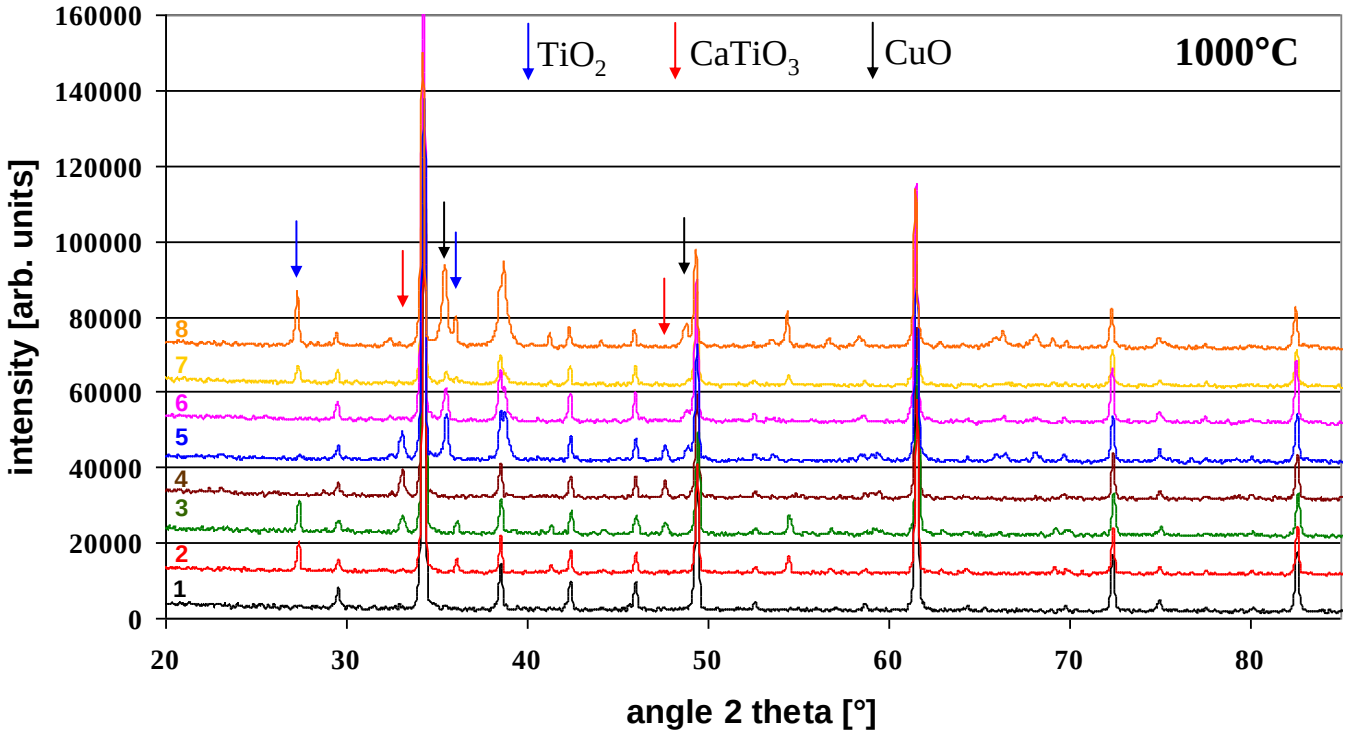

SM Figure 1 Powder XRD patterns of compositions 1 - 8 fired at 1000 ºC. Blue, red and black arrows correspond to the most intense TiO_2, $CaTiO_3$ and CuO reflections respectively. CCTO reflections are not indexed.

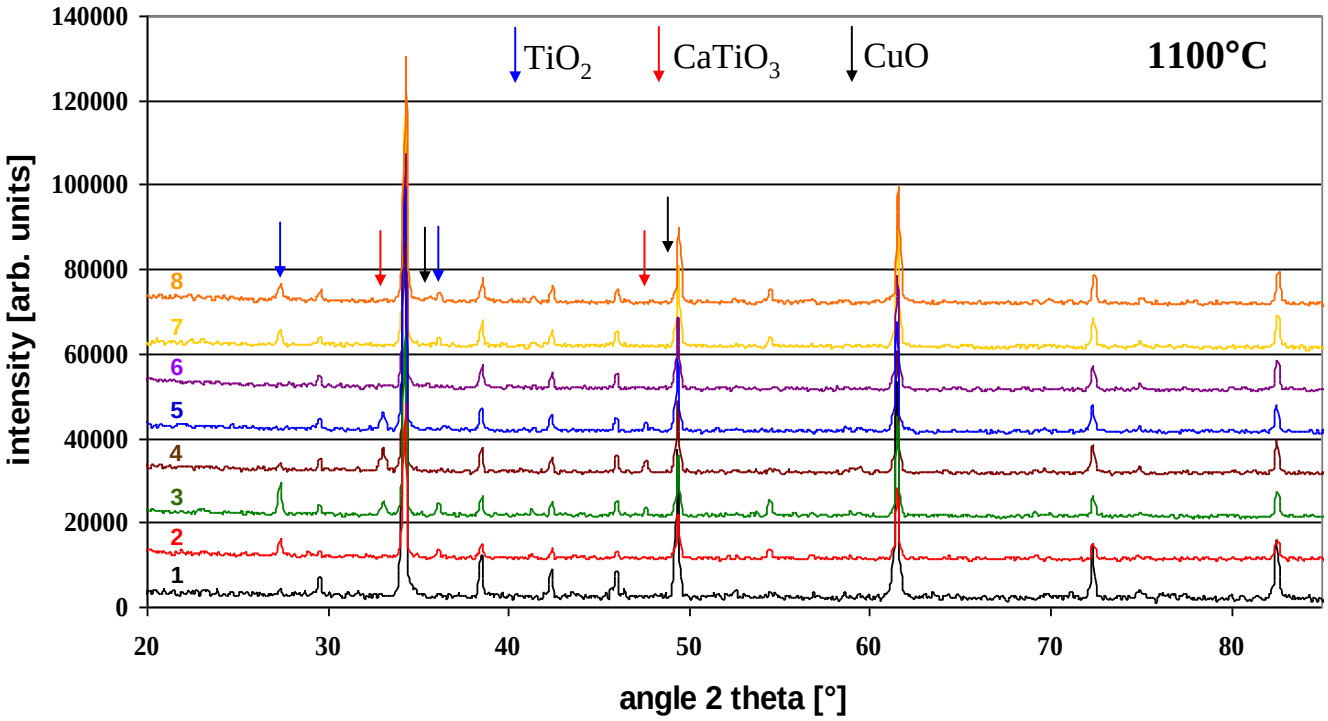

SM Figure 2 Powder XRD patterns of compositions 1 - 8 fired at 1100 ºC. Blue, red and black arrows correspond to the most intense TiO_2, $CaTiO_3$ and CuO reflections respectively.

All phase compositions are in agreement with expectations from the phase diagram (Fig.1 main text) for the 1000 ºC samples. In the case of 1100 ºC heat treatment the CuO phase is missing for all compositions. In the main text it was argued that CuO may partially melt and segregate, or remain amorphous after re-solidification upon cooling. A further possibility may be Cu volatilization.

(b) Phase analysis by Scanning Electron Microscopy (SEM)

SM Figure 3 shows images of 1100 ºC fired pellets of all compositions 1 - 8 using SEM operated in the secondary electron (SE) mode. The microstructure for different compositions was

investigated and the expected phases are indicated for each image. The different extra phases present in different compositions may lead to slightly different sintering behavior and to the observed differences in the grain microstructure.

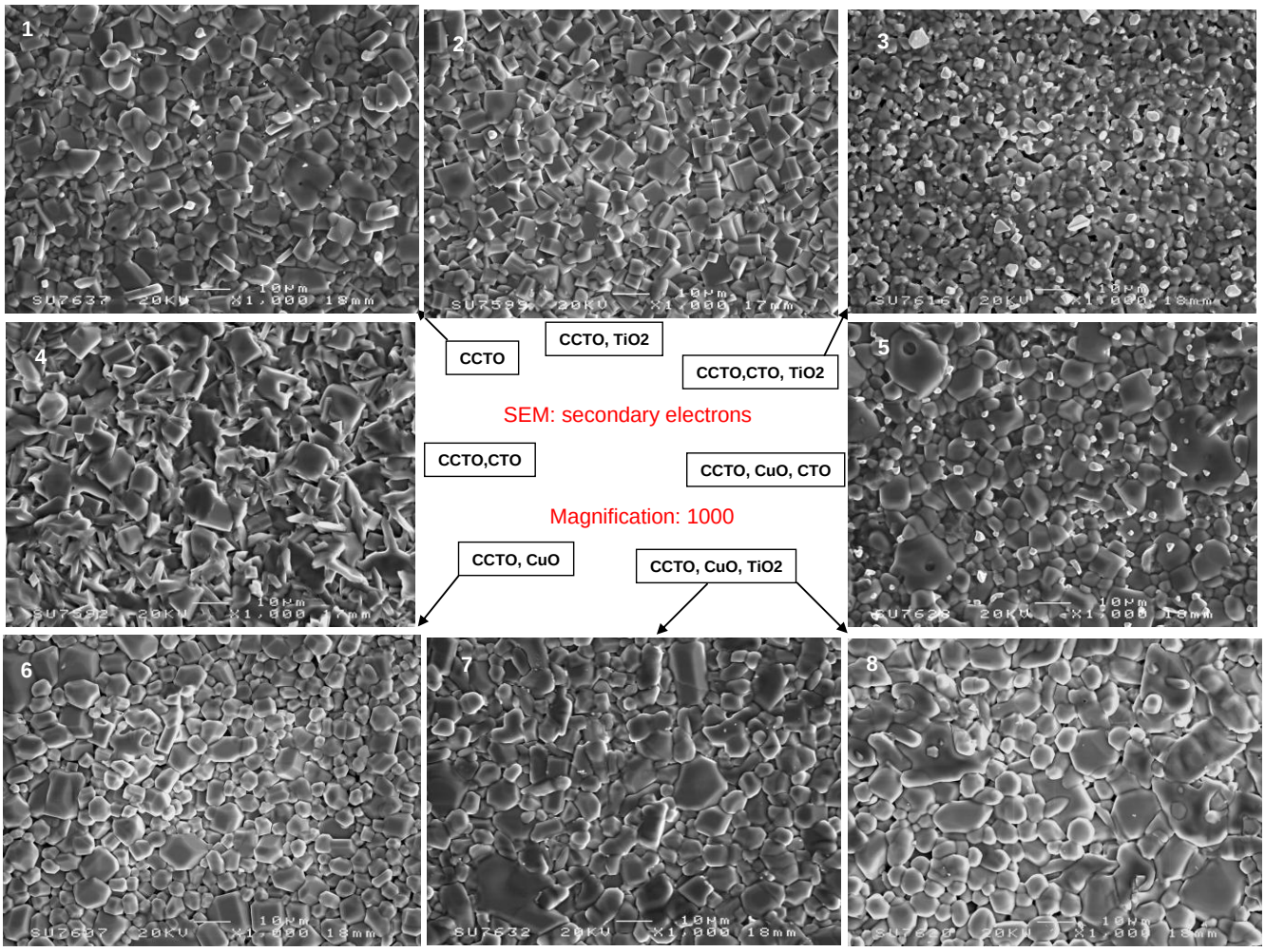

SM Figure 3 SEM micrographs collected in the SE mode for 1100 ºC sintered pellets of compositions 1 - 8, magnification x1000. The phases expected from the phase diagram (Fig.1 in the main text) are indicated.

SM Figure 4 shows images of the same but polished pellets as SM Figure 3 using SEM in the backscattered electron (BE) mode. The contrast in the BE images gives clear indications of the different phases present. Phase identification was carried out using quantitative focused electron

spot EDAX. The electron beam was focused onto single grains and the quantitative analysis yields unambiguous evidence for each phase present. For example, focusing the electron beam on a TiO_2 grain gives EDAX results of Ca 0.57% : Cu 1.19% : Ti 98.24% (at.%) cation ratio (blue arrows). A typical CTO grain yields Ca 44.26% : Cu 3.12% : Ti 52.62% (red arrows). A peculiar but significant Ti excess is detected in all CTO grains. CCTO grains showed the expected ratio of about Ca 12.67% : Cu 36.93% : Ti 50.40% within experimental error.

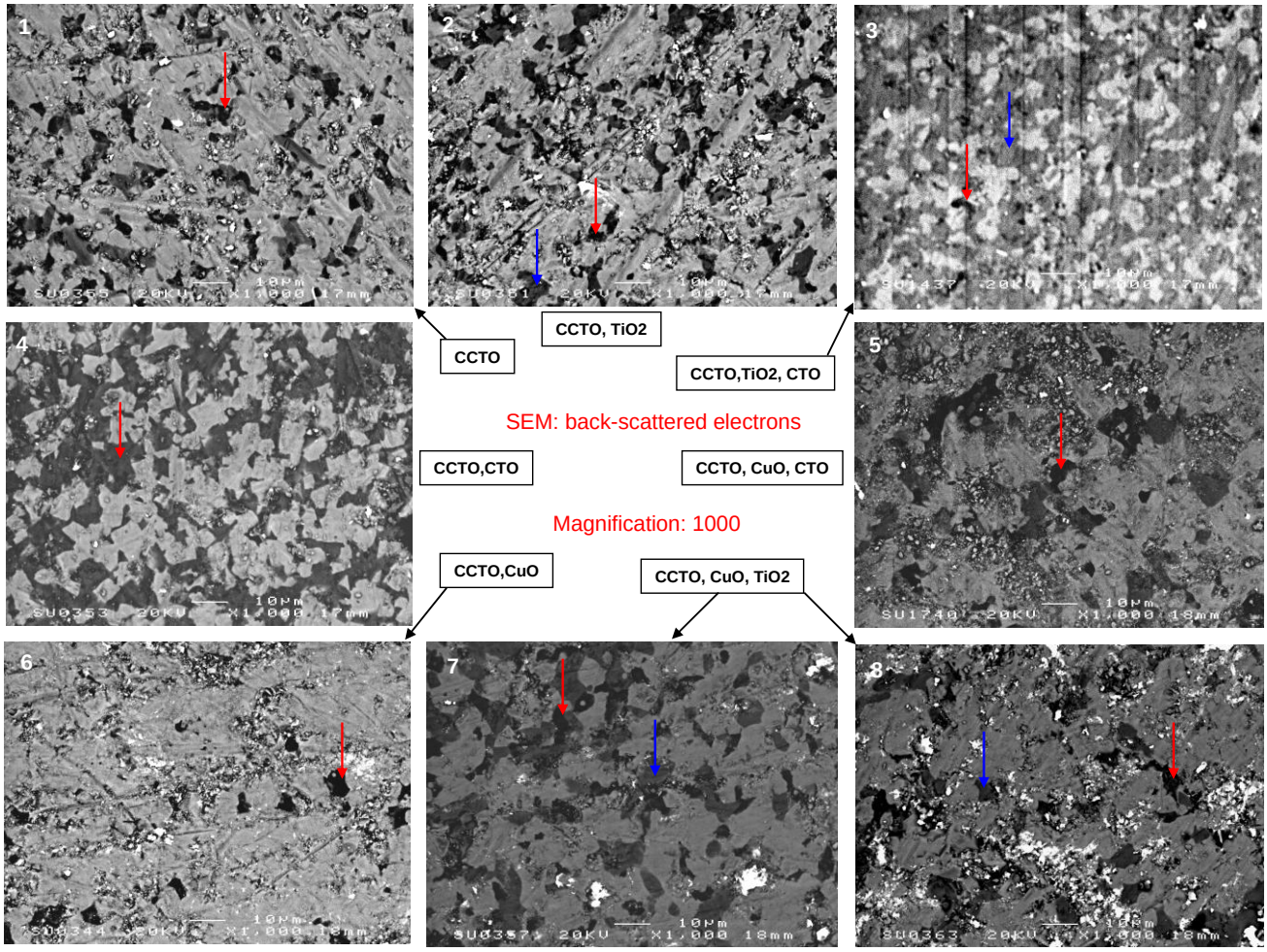

SM Figure 4 SEM micrographs collected in the BE mode for 1100 ºC sintered pellets of compositions 1 - 8, magnification x1000. The phases expected from the phase diagram are indicated. Blue arrows ↓ correspond to TiO_2, red ↓ to $CaTiO_3$, all remaining areas are CCTO.

No clear CuO regions could be detected, but small unexpected amounts of CTO grains in several compositions. In the main text it was suggested that this may be a consequence of Cu loss due to partial melting. In composition 4 signs of CTO were exceptionally small (see table I, main text). The very bright (white) spots in SM Fig.4 for compositions 7 & 8, and less significantly in compositions 5 & 6, are Ag residues. Quick drying Ag paste had been used to mount the pellets for SEM .

(c) Scanning Tunneling Microscopy (STM)

In order to demonstrate partially melted CuO, STM measurements were carried out on the surface of pellet composition 6 (SM Fig.5). The bright regions on the pellet surface (black arrow) correspond to a conducting Cu-rich phase. The amount of conducting phase shown is small and disappears upon polishing. Therefore, full percolation of the Cu-rich phase can be excluded.

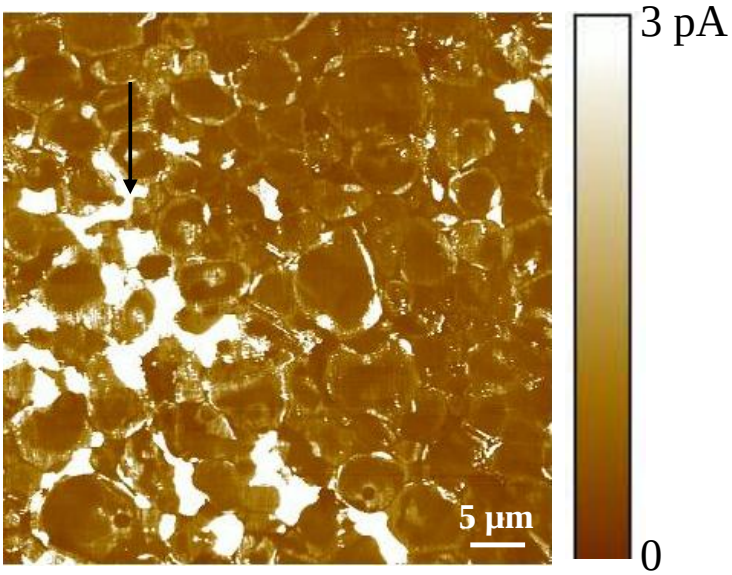

SM Figure 5 STM analysis of 1100 ºC sintered pellet of composition 6. The image contrast reflects differences in conductivity. The black arrow points on a bright contrast area of a Cu containing conducting phase.

II. Analysis of impedance spectroscopy data using ε' vs f and M'' vs f plots

a) Impedance spectra from Cu deficient compositions 1 - 4

The impedance spectra of compositions 1 – 4 all display 3 relaxations, which can be associated with the intrinsic bulk, GB and electrode contributions. As a representative example, composition 3 was chosen and the 3 relaxations are evidenced at different temperatures by 3 permittivity plateaus in ε' vs f (SM Fig.6a) or by 3 relaxation peaks in M'' vs f (SM Fig.6b) plots.

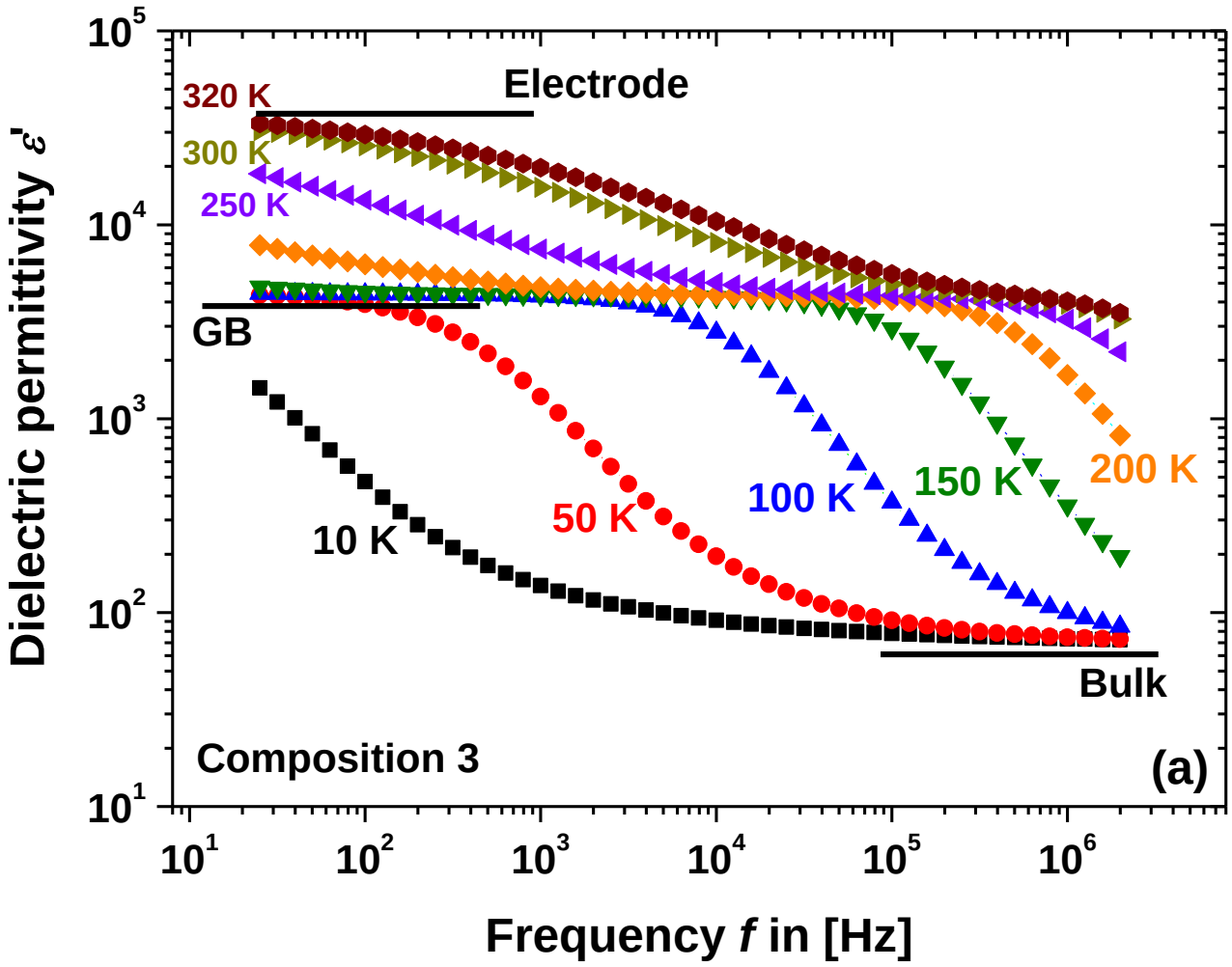

SM Figure 6a ε' vs f for composition 3 at various temperatures. The different types of relaxation plateaus are indicated by solid black lines.

The electrode relaxation can often be distinguished from the GB contribution, if it exhibits non-ohmic electrode resistance. This is usually the case in CCTO and it was interpreted as a Schottky barrier forming at the electrode-sample interface due to mismatching work functions of the electrode material and CCTO. The data presented are typical for CCTO ceramics and agree well with previous reports. The behaviour presented in SM Fig.6a/b is indicative of 3 dielectric relaxations represented by 3 RC elements in series in an equivalent circuit.

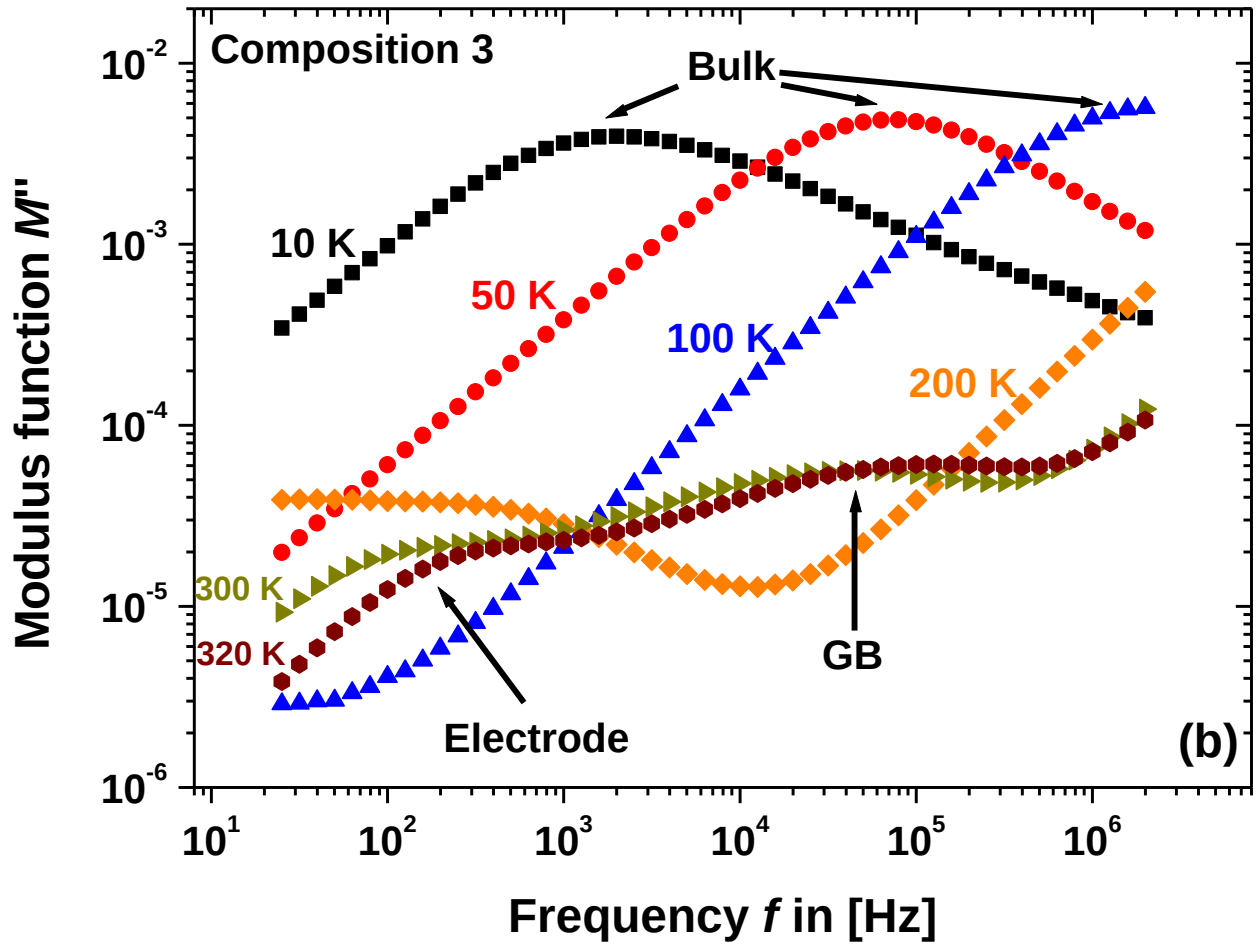

SM Figure 6b M'' vs f for composition 3 at various temperatures. The different types of relaxation peaks are indicated by arrows.

The behaviour for composition 3 (containing CCTO as a main phase and TiO_2 and CTO as secondary phases) is qualitatively similar to the results for compositions 1, 2 and 4. The addition of TiO_2 and CTO secondary phases only slightly changes the dielectric response of CCTO in a quantitative way.

b) Impedance spectra from compositions 5 – 8 containing secondary CuO

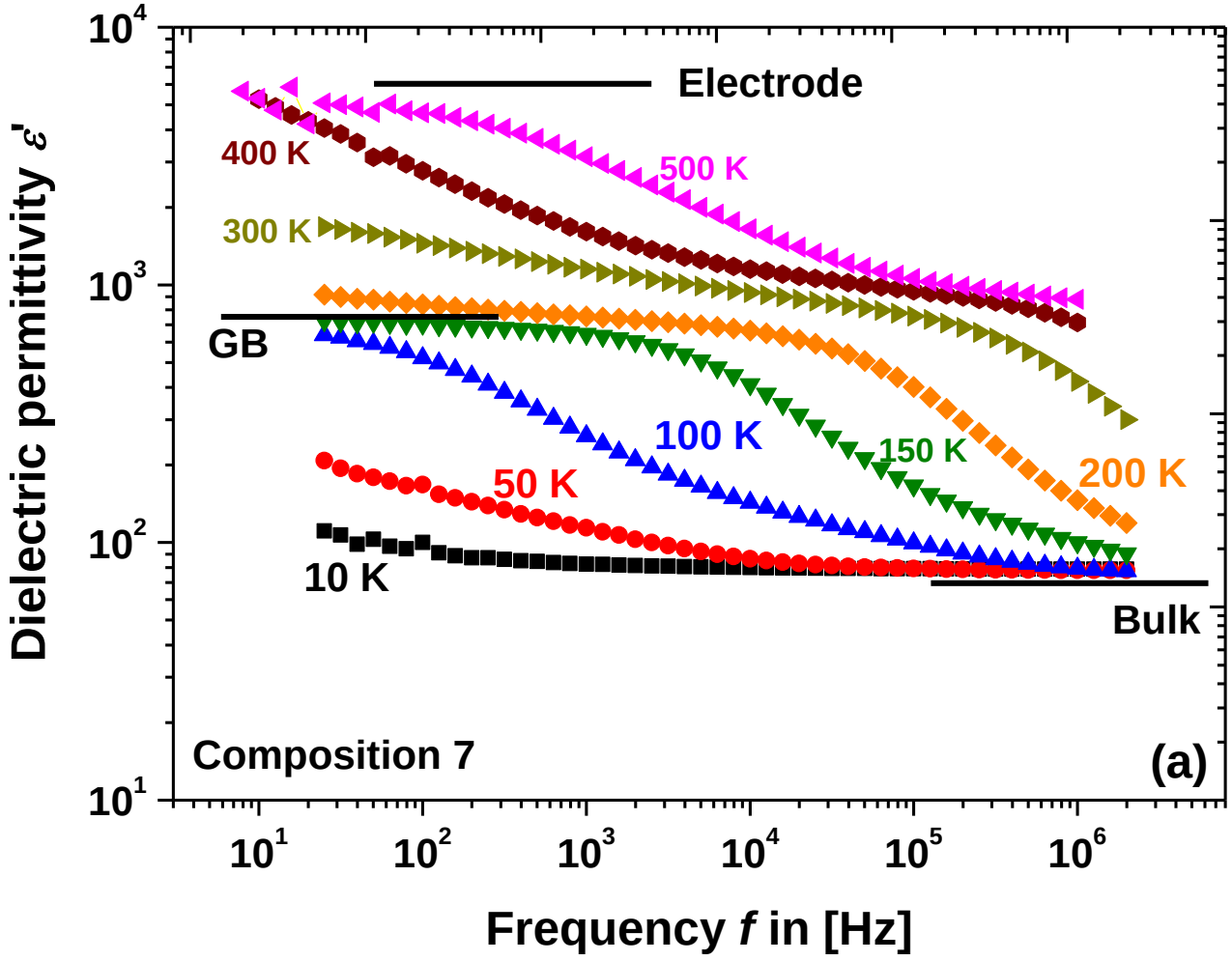

SM Figure 7a ε' vs f for composition 7 at various temperatures. The different types of relaxation plateaus are indicated by solid lines.

In the main text it was pointed out that the CuO containing composition 5 displays equivalent dielectric response as 1 – 4, possibly due to a low Cu concentration, whereas 7 & 8 are clearly different. Therefore, composition 7 was chosen as a representative example showing the effects of secondary CuO and the ε' vs f and M'' vs f plots are shown in SM Fig.7a/b. The differences between bulk and GB permittivity in 7 (SM Fig. 7a) are less distinct as for 3 (SM Fig.6a), and it may be concluded that the bulk and GB relaxations are more similar to each other in composition 7.

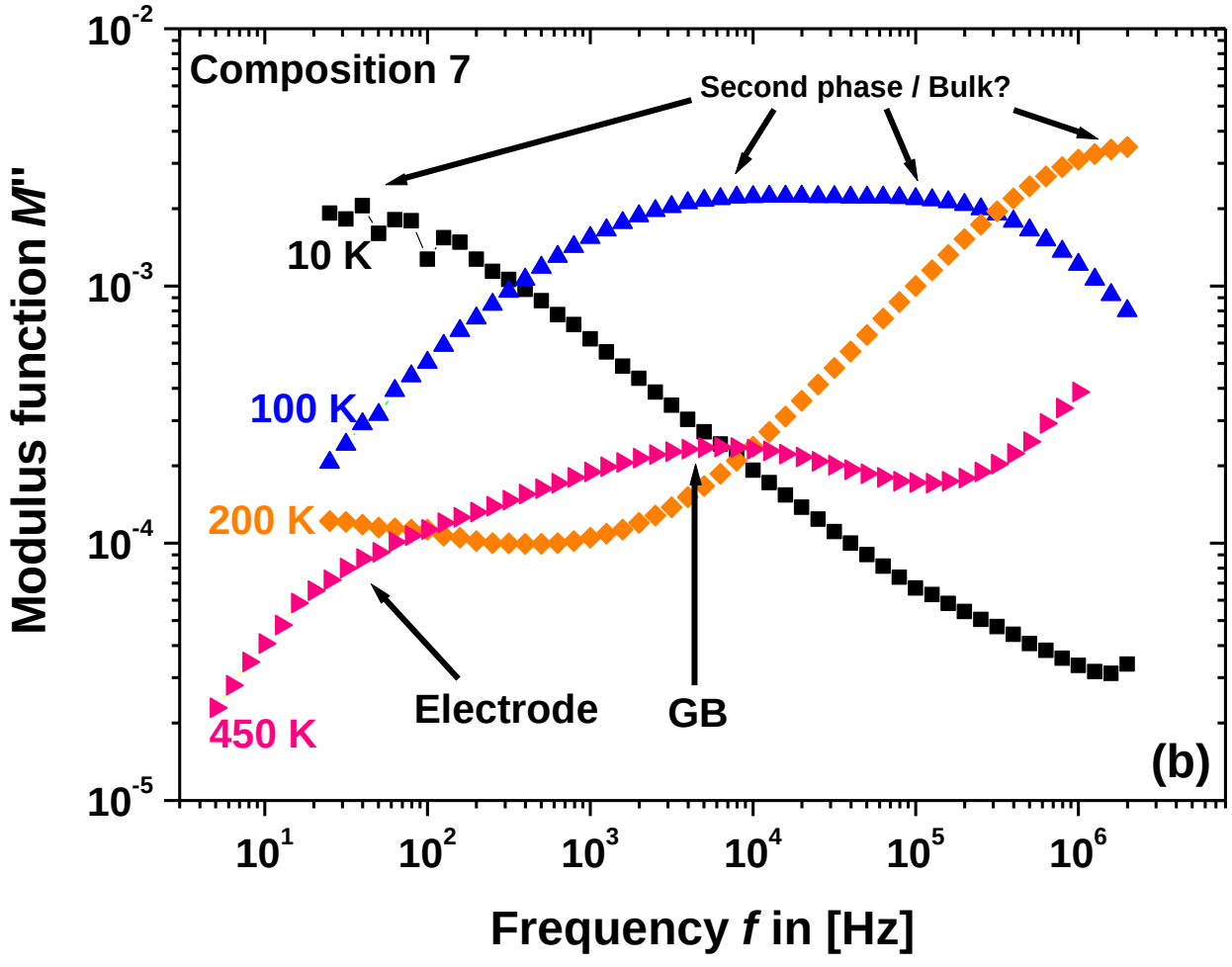

SM Figure 7b M'' vs f plots for composition 7 at various temperatures. The different types of relaxation peaks are indicated by arrows.

The bulk relaxation peak in M'' vs f plots (SMFig.7b) shows distinctively different features as compared to compositions without CuO, whereas the GB and electrode relaxation peaks are rather similar in 3 & 7. All relaxation peaks for 7 occur at lower f (or higher temperature) as a result of the generally higher resistivity. The origin of the bulk relaxation double peak structure in 7 (SM Fig.7b/main text Fig.2b) is unclear. As mentioned in the main text, different scenarios are possible:

Scenario (1): A second separated secondary phase such as CuO may be present. Such CuO related secondary phase would occur in small quantities, because no percolation occurs as is argued in the following. In case of high amounts of CuO either percolation would lead to a dielectric response totally dominated by the secondary phase, or the secondary phase would be completely by-passed (depending on the resistivity). Both scenarios are clearly not indicated in SM Fig.7b. The secondary phase is clearly visible in addition to the CCTO-type GB and electrode relaxations. Since the possibly Cu-related secondary phase is not completely bypassed it needed to exhibit lower resistivity as compared to the CCTO grains.

This scenario may be unlikely, because in compositions 7 & 8 no secondary CuO-like phase is visible by XRD and backscattered SEM, and CuO seems likely to have melted completely and precipitated out of the samples.

Scenario (2): The bulk double peaks in SOM Fig. 7b and Fig.2b in the main text could potentially indicate the presence of two impurity phases and the CCTO bulk relaxation peak is absent. This is quite unlikely, because XRD and backscattered SEM again do not indicate secondary phases in 7 & 8. The CCTO bulk resistivity would be massively increased to be completely bypassed and needed to be higher than the resistivity of the low frequency bulk-type relaxation peak.

Scenario (3): Two CCTO type bulk relaxations may occur. This would imply that the bulk CCTO material is inhomogeneous, possibly due to an inhomogeneous and bi-modal distribution of the Cu content, i.e. one Cu-deficient and one Cu-rich phase may co-exist. It is interesting to note that the ratio of the peak height of the two double-peaks varies for composition 7 & 8 (main text Fig.2b, Inset). In 7 the high-*f* peak is larger (i.e. indicating smaller capacitance), whereas in 8 it is the low-*f* peak that is larger. This discrepancy could be explained by a geometrical effect, where the peak height ratio (i.e. ratio of the capacitance) may depend on the amount of the different CCTO phases present. The geometrical factor of each CCTO phase may be modified and the measured bulk capacitance of primary CCTO and secondary CCTO would vary accordingly as indicated by the varying peak heights. This scenario seems most likely and is consistent with the notion that the Cu content in CCTO strongly influences the resistivity.

Although Scenario (3) is favoured here, it still remains unclear whether there really exist two types of CCTO grains with different electrical properties in compositions 7 & 8. What seems to be clear is that the electrical microstructure in CCTO ceramics is always based on a core-shell model with a certain variation of Cu-content between outer and inner regions of individual grains.